

Contributions to Colon Segmentation Without Previous Preparation in Computer Tomography Images

Darwin MARTINEZ
Los Andes University -IMAGINE
Colombia, Bogota, D.C.
dar-mart@uniandes.edu.co

José Tiberio HERNANDEZ
Los Andes University -IMAGINE
Colombia, Bogota, D.C.
jhernand@uniandes.edu.co

Leonardo FLOREZ
INSA-Lyon - CREATIS
France, Lyon
leonardo.florez@gmail.com

ABSTRACT

We propose a method to segment the lumen of the colon from computed tomography (CT) images. To do so, we use first and second order statistical moments. These moments provide us with a set of descriptors to characterize the homogeneity of regions inside the colon.

The algorithm presented in this paper makes use of these values in a prediction-correction exploration process of the colonic region. We show some segmentation results on real patient images that present high non-homogeneous colonic regions.

Keywords

Segmentation, virtual colonoscopy, image processing, statistical moments, variance, image descriptors, region growing, prediction-correction.

1. INTRODUCTION

Colorectal cancer is one major cause of death in the western world [6,7,13]. This disease is less risky if the polyps that cause it are detected in early stages [3,5,7,12,13,18,20,28]. Virtual Colonoscopy (VC), a digital method for polyp detection, is widely accepted because it is less invasive than optical colonoscopy[21].

VC procedure consists on the acquisition of an air-contrasted Computer Tomography (CT) 3D image. This image is then analyzed to identify possible deformations of the colon wall. Analysis is performed by an expert radiologist who uses computer based diagnostic tools specially conceived for:

- colonic lumen segmentation,
- colon central axis computation, and
- polyp detection.

Firstly, the segmentation process is implemented as a threshold filter based on the CT Hounsfield Units

Permission to make digital or hard copies of all or part of this work for personal or classroom use is granted without fee provided that copies are not made or distributed for profit or commercial advantage and that copies bear this notice and the full citation on the first page. To copy otherwise, or republish, to post on servers or to redistribute to lists, requires prior specific permission and/or a fee.

Copyright UNION Agency – Science Press, Plzen, Czech Republic.

(HU) [11]. These units represent different structures in a standardized scale: air has a value between -1000 HU and -800 HU [5,20,29]. The main problem of a simple threshold is the presence of adjacent organs in the abdominal region: lungs, stomach and small intestine are also filled with air, thus faking the segmentation results. In such cases it would be necessary to use more elaborated strategies to extract the colon and eliminate adjacent structures. The most common strategies are often based on region growing. The user provides a seed set inside the colon and the growing algorithm is adapted to avoid adjacent regions. Some examples of these procedures can be found in [1,2,4,5,12,14-17,20,23,28-30].

Secondly, axis computation is often based on morphological erosion [22] or on the analysis of a distance map [11,28]. Such geometrical object is used as a navigation path, inside the colonic lumen, to guide detection of polyps [22,28].

Finally, detection of polyps is not an easy task. Most methods use a hybrid approach to coarsely detect polyps and then refine this detection. Subsequently, specific rules are applied in order to classify detected regions as polyps.

Some techniques used for polyp identification are:

1. Geometric characterization: different properties such as elliptic curvature, mean curvature, minimum size [1,25], diameter, sphericity [26,27], height, radius, mean intensity[14] are measured. These measurements are affected by the colon distention, resulting from air insufflations.

2. Density characterization: the uniformity of voxel sets identified as polyp candidates in the previous process is studied [26].
3. Deformable models: starting with a selection of identified polyp candidates, this technique places a seed inside each candidate. The model grows until it reaches the surface of the polyp [30].
4. Optic flow: this process evaluates the differences between the edges of polyp candidates (identified by means of geometric characterization in the previous stage) in adjacent slices.

These techniques intend to emulate the method used by the experienced radiologist without computer aid [1,2].

Segmentation is a fundamental part of the process. The quality of polyp detection in the VC procedure depends on the precision of the segmentation stage, both if the detection is performed by the radiologist and if the above mentioned techniques are used.

Motivation

In order to reduce patient preparation and the invasive characteristics of air contrast VC, we propose to explore the behavior of some segmentation image processing techniques in CT studies of patients with less or no preparation. A particular study of variance

as region descriptor [10,19,24], and the region explorers based on the prediction-correction technique[9] was made. It's important to mention that the present work does not have clinical intention and it is just an exploration of an alternative segmentation method.

Our method proposes working over a 3D image whose values are the variance of the intensities in the original image computed in each voxel's local neighborhood. We intend to explore the local homogeneity of the colon content (air and feces matter) as a main criterion in segmentation, and the original data as validation parameters in the region growing process.

The method is an interactive process of prediction-correction, using an advance strategy based on an initial vector provided by the user, and a prediction instrument (explorer's set) which guides the process along the colon.

Results show a good behavior both of the variance as workspace for this kind of segmentation, and of the advance strategy along the colon.

2. METHODOLOGY

The selected segmentation strategy is composed by two stages:

- Preprocessing and Initialization
- Iterative Segmentation

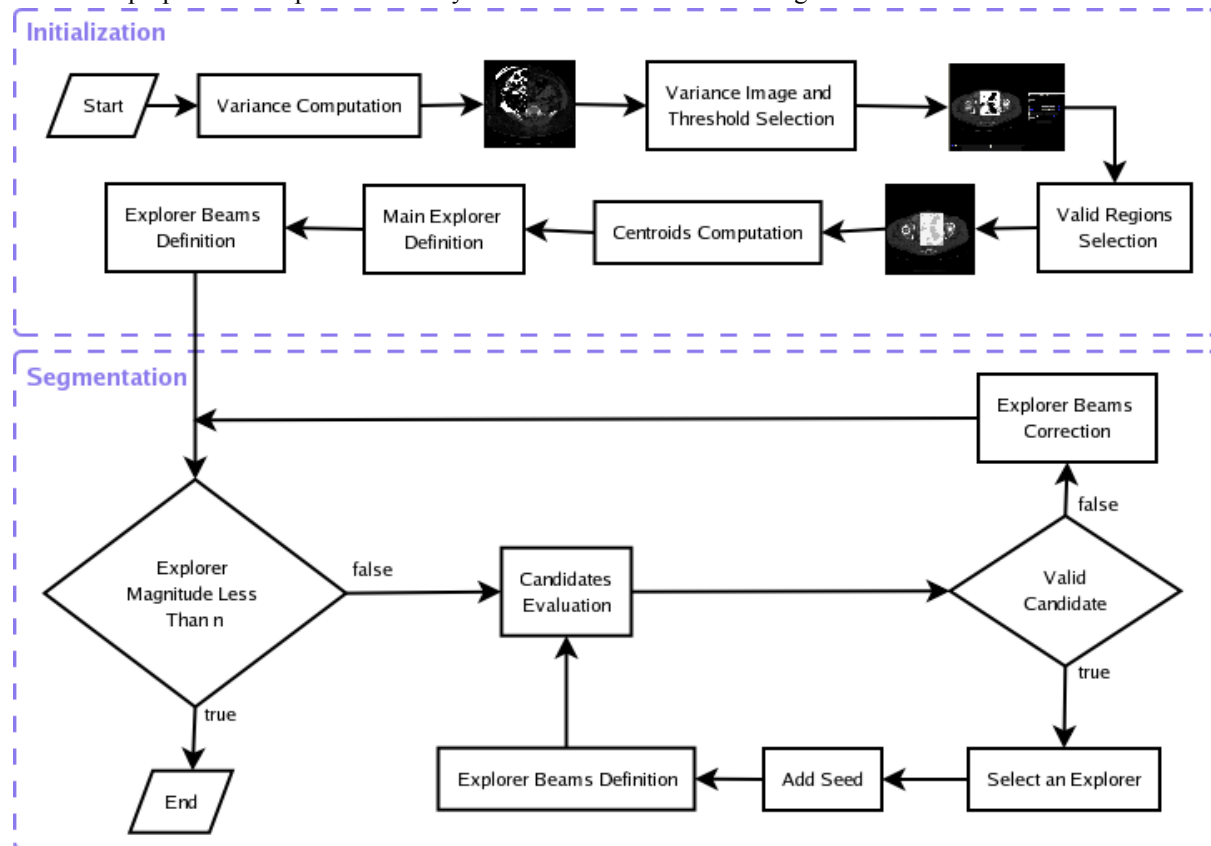


Figure 1: Procedural Flow Diagram

In the preprocessing and initialization stage the *variance image*—starting from the local variance values of the original image—is built using a neighborhood size parameter (between 5 and 11 voxels) defined by the user, who also defines a threshold (in the *variance image*) characterizing the regions inside the colon wall (air and feces matter). The user then defines the first *advance vector*, which must have the origin and end points in the two different valid and adjacent regions.

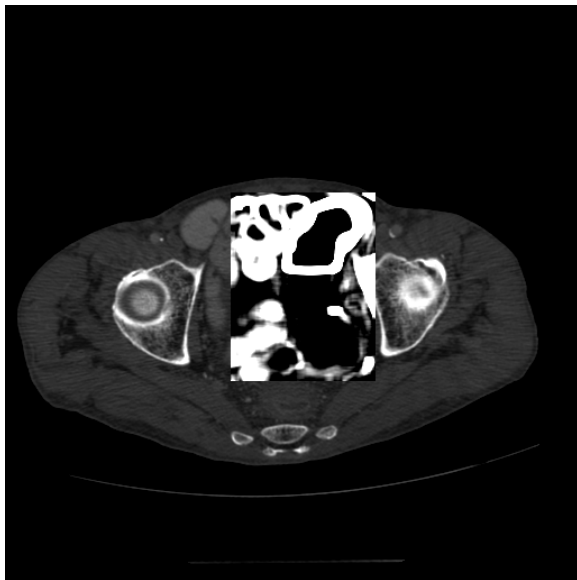


Figure 2: Preprocessed Image. Chess representation of variance on original image. Variance was calculated with a cubical kernel of 7 voxels of side.

The segmentation stage is an iterative process based on the prediction-correction algorithm. In our case, this algorithm uses the *direction vector* of the last iteration as a guide for advance (prediction). An *explorer beam* (EB)—data structure composed by a set of vectors surrounding one main direction and providing associated image information—is used to explore and evaluate the region in order to define a new *direction vector* (correction) and thus launch the growing process. The stop criterion is the failure of the new direction vector search.

Preprocessing and Initialization

2.1.1 Computing the Variance Image

The 3D image preprocessing is based on the computation of the mean and variance values for all the voxels inside the user-selected volume of interest (VOI). This procedure generates two new images, one for the mean and another for the variance values. The selected VOI should contain the two valid regions inside the colon (air and feces matter). The variance values in 3D are computed in the traditional way. It is important, nevertheless, to consider that, when a voxel

neighborhood is not completely contained in the VOI, the formula should be modified to exclude outside voxels.

2.1.2 Defining Region Growing Threshold

The user selects a threshold on the *variance image*, for which purpose the system offers an interactive visualization of original and variance VOI images. The threshold should be chosen in a way such that in the *variance image* the colon wall (high variance) and the different regions inside the colon (rather low variance) are clearly seen, especially those with feces matter. Also, in some occasions it is difficult to distinguish between the outside of the colon wall and the wall itself.

2.1.3 Selecting Valid Regions

As previously mentioned, the procedure requires the identification of two valid and adjacent regions inside the colon, one with feces matter and the other with air. In order to facilitate the selection of valid regions, the system provides an interactive visualization of both the original and the chess variance VOI images.

Each selected region—an interior parallelepiped—is used as a characterization frame of the regions, expressed in the variance and the mean behavior. The behavioral descriptors are the main parameters for both explorer evaluation and region growing steps. These last steps are based on the variance and intensity gray values of each voxel in the image and they define the validity characteristics for the regions.

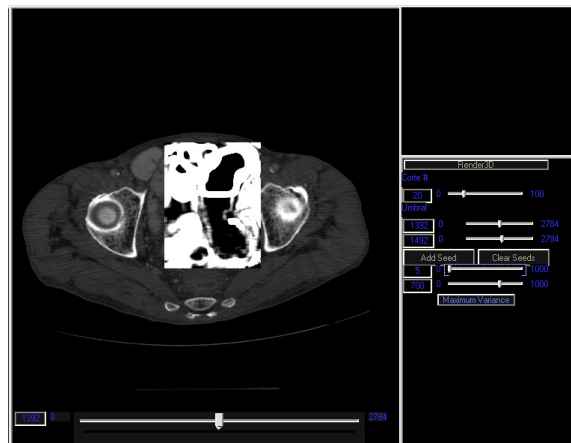


Figure 3: Threshold variance manipulation to evidence the differences between regions inside and outside colon. Particularly, it shows the homogeneity of region variance for both kinds of regions inside colon.

Once a valid two regions selection has been performed, the procedure defines an initial *direction vector*, the first main explorer. This explorer is specified by the magnitude and direction as follows:

1. Computing the regions' centroids,
2. Computing the distance between centroids,

magnitude

3. Defining the direction based on the order of region selection.

The final point of this vector will be the first seed for the region growing, which starts the segmentation process.

2.1.4 Defining the Explorer Beam

The *explorer beam* (EB) is a set of vectors used to guide the advance in the segmentation process. The method creates the EB based on direction and magnitude of the previously selected *direction vector*.

Let us define the main explorer of the EB e_p as the vector that has the same magnitude and direction of the previous *direction vector*. Its origin is the end point of the previous *direction vector*. Other explorers in the EB are created around e_p in a way such that a cone with an alpha angle is formed whose vertex is in the origin point. The result is an explorer semi-conic beam. So, the EB would be view as a data structure to search for some characteristics of image as gray value and variance along each vector around e_p .

In other words, for each new vector in EB, the procedure computes the variance all along, so that a variance profile of each explorer is created. This profile is used in the explorer's evaluation (section 2.2.1).

Iterative Segmentation

2.2.1 Evaluating the Explorer Beam

The evaluation verifies the existence of a valid vector candidate in the explorer beam, according to the following validity conditions:

1. The variance values associated to the vector voxels are in the valid range defined by the selected valid regions, and
2. The corresponding intensity values are within the valid range defined for the same valid region.

The algorithm searches for explorers that comply with the above conditions. If e_p is among them, it should be selected. The final point of the selected explorer will become a seed for the region growing stage (section 2.2.4). In the event that no explorer in the current EB fulfills the conditions, the correction step begins (section 2.2.2).

2.2.2 Correcting the Explorer Beam

The objective of this step is to find a complying explorer beam which should contain the next direction vector. The correction uses two different control variables: the magnitude of vectors and the direction of the main explorer (*direction vector*). Even though the conic angle might be used as another control variable, it was not pursued in this study.

When an explorer fails the evaluation step, each of its vectors is labeled with the value of the distance from its origin to the first non-compliant voxel (fail label). The EB correction is calculated from the explorer's fail label distribution, and it proceeds in two different ways:

1. Magnitude correction: the magnitude of all explorers is reduced in half. This correction takes place when the fail labels have similar values.
2. Direction correction: a new main explorer is created by using the explorer with the greater fail label, whose direction will correspond to that of the new main explorer. The new main explorer's magnitude will correspond to the fail label value of the very same explorer. This correction takes place when the fail labels have fairly different values.

This new EB demands a new evaluation process (section 2.2.1).

2.2.3 Stop Criterion

The exploration cycle stops when, after an EB correction, the magnitude of vectors is found to measure less than one unit.

2.2.4 Region Growing

The region growing is started at the end of each iteration. It takes as seed the end of the selected explorer (the new direction vector). This propagation is a recursive method that evaluates the 6-orthogonal neighbors seeking for the voxels that fulfill one of the following two conditions:

1. The estimated variance value for the voxel is in one of the ranges of valid variance,
2. The voxel has an estimated variance smaller than the threshold specified in the initialization stage, and its gray intensity is in the valid range of intensities.

When a voxel fulfills one of the conditions, it is singled out, and the region follows. The algorithm stops when no voxel fulfills at least one condition.

3. RESULTS

Next, presenting the image homogeneity conditions that shows a good results.

Figure 4 shows two graphics showing the manipulation of variance threshold estimation, which enhances the image characteristics in a chess representation of statistical values on top of the original ones, the a) figure shows an image of the colon with a good homogeneity in the feces matter region, while the b) figure shows an image with high variance in the feces matter region, so the image does not keep the hypothesis of low variance in the regions inside the colon, and for this reason the image were

discarded. Figure 5a presents a variance image where the influence of two types of scenarios becomes evident: the transitions between air and organs, and that between organs and organs. Figure 5b illustrates the appearance of a border in the feces matter region inside the colon. This image is obtained through the manipulation of the variance threshold. Finally, figure 6 shows the method's results in a fragmented segmentation of the matter inside the colon.

The procedure was applied to four different CT

images. These images present different characteristics in region homogeneity inside the colon. All images present an oral contrast medium that lightens the small intestine. Two of these images have homogeneous regions inside the colon with an insufficient size for estimator computation in the initialization stage. In this case, the process did not achieve reliable estimators, and the images were discarded.

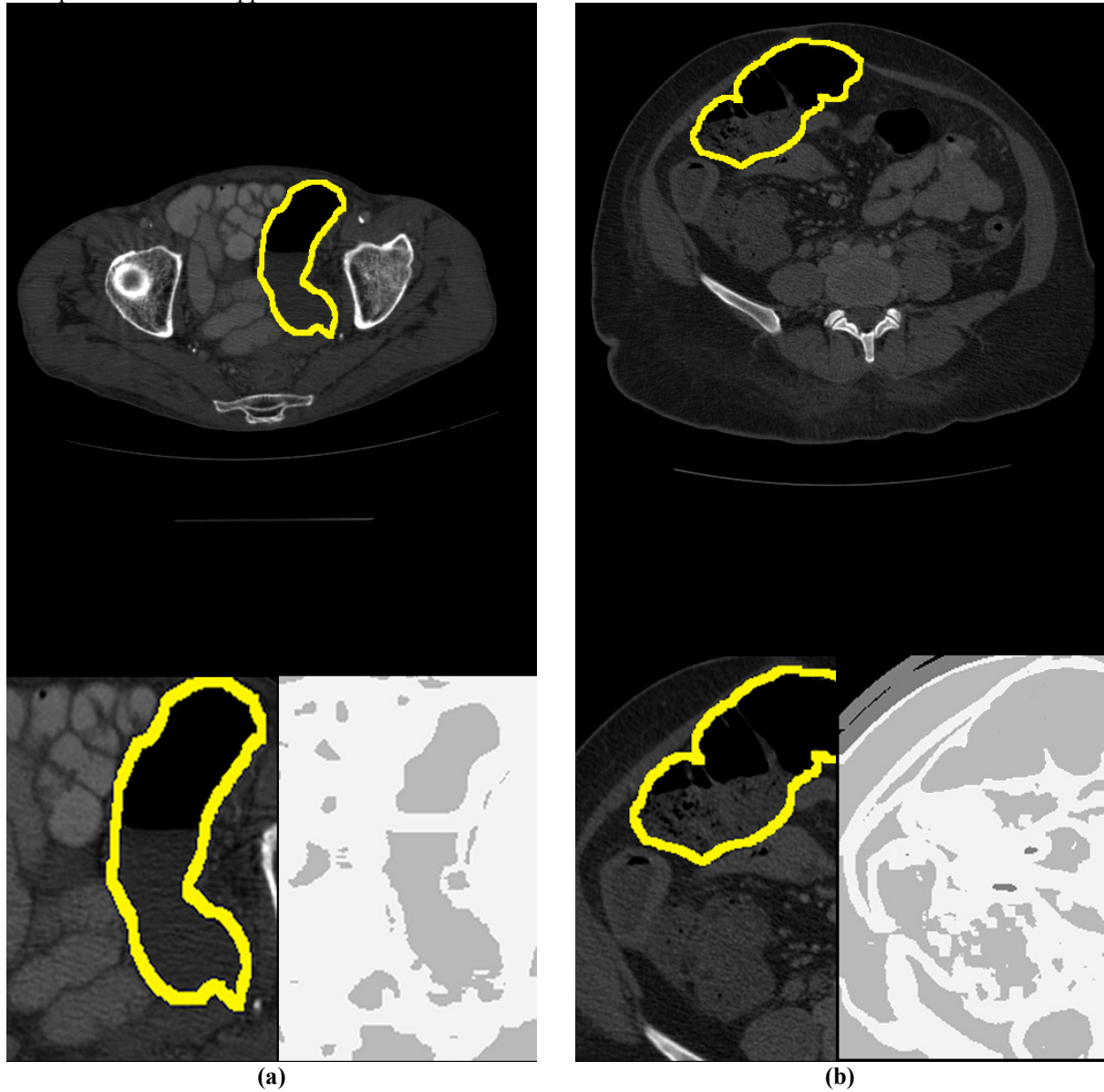


Figure 4: Variance manipulation: the yellow highlighted regions correspond to the colon wall, In both cases they represent the region to segment. a) homogeneous regions inside the colon present low variance b) non homogeneous regions present high variance. It is important to note that image a) fulfills the hypothesis of continuity based on variance while image b) does not.

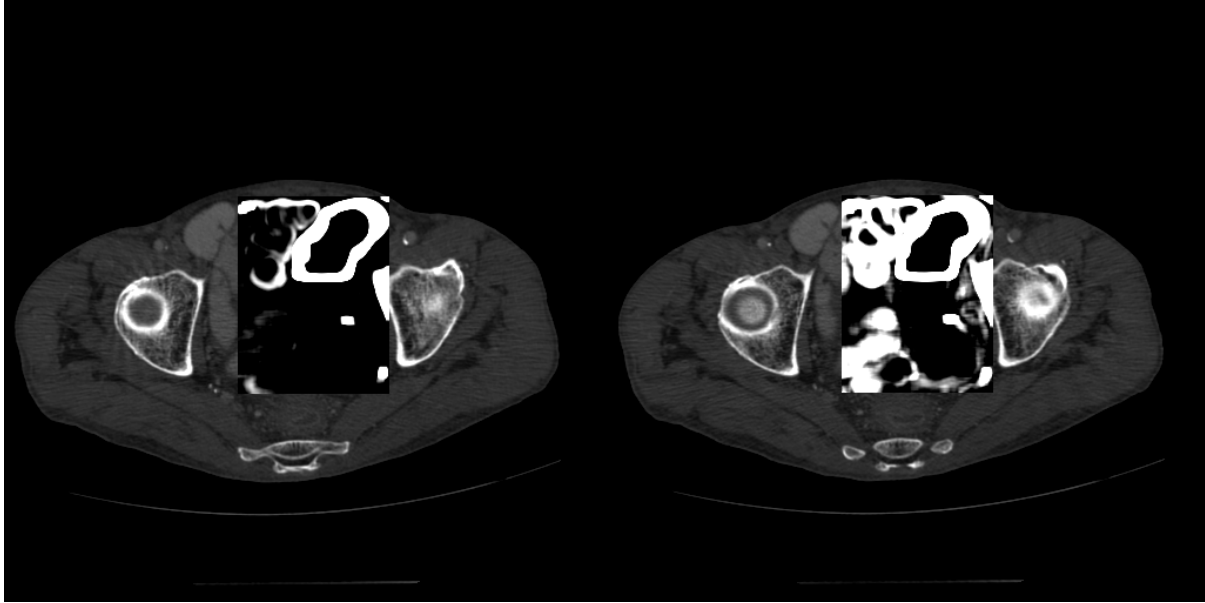


Figure 5: Interactive variance threshold manipulation: The choice of this threshold is critical for the method. In the left side image, a very high threshold hides the relatively low variances of fecal matter, while a lower threshold (right side image) allows the visualization of the internal region of colon (air and fecal matter), surrounded by high variance regions in organs around the colon. In this way, the image of the right side is appropriate for the interactive definition of the two seeds for the segmentation process.

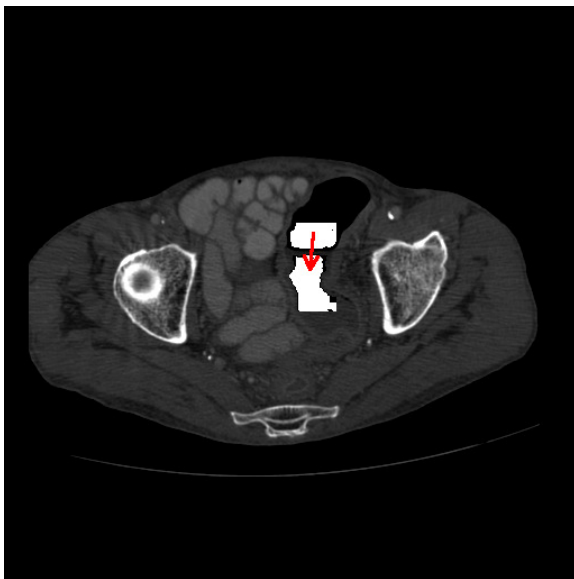


Figure 6: A chess representation resulting from the segmentation of regions inside the colon. We can see two white fragments that represent the segmentation in the two valid regions over the original image. The segmentation follows the direction of the red arrow (starting at the first direction vector).

4. DISCUSSION AND CONCLUSION

The variance as image regions descriptor gives a good estimation about the region's homogeneity. Statistical

3D computation gives a space continuity condition for the matter. Figure 4 shows two cases where the variance enhances the homogeneity conditions in the regions inside the colon. In a) this condition is particularly notorious, while in b) the region inside the colon shows high variance. In this case, the estimation of regions inside the colon could be misleading because responses to transitions between organs might interfere. This is the reason why these images were discarded. Figure 5 presents two variance images. The first one shows higher variance obtained as a response to changes in the distribution of intensity gray values corresponding to different organs, and to air and osseous structure.

Additionally, the second image indicates how a fragment of the wall is lighter as a response to the influence of the changes in adjacent slices. This determines the threshold condition for the region growing.

In conclusion, we find that the statistical descriptors offer a good estimation of region homogeneity that includes the spatial distribution. Also, the strategy of prediction-correction facilitates the algorithm's easy adaptation to image conditions using local values both to determine the advance direction, and to act as reference values in the region growing process. Additionally, we find an enormous utility in expressing the decision criteria in the region growing process based on more than one characteristic (the variance, mean, and original images) to evaluate the growing conditions.

Based on the proposed sketch, explorer beams evidence a good potential for other applications. A further study of the stop criterion and the correction strategies previously mentioned would be an important development.

5. REFERENCES

- [1] B. Acar, C.F. Beaulieu, D.S. Paik, S.B. Göktürk, C. Tomasi, J. Yee, S. Napel, Assessment of an Optical Flow Field-Based Polyp Detector for CT Colonography, in 23rd Annual International Conference of the IEEE Engineering, 2001.
- [2] Burak Acar, Christopher F. Beaulieu, Salih B. Göktürk, Carlo Tomasi, David S. Paik, R. Brooke Jeffrey, Jr., Judy Yee, and Sandy Napel, Edge Displacement Field-Based Classification for Improved Detection of Polyps in CT Colonography, in Medical Imaging IEEE Transactions, 2002.
- [3] American Gastroenterological Association, Cancer Colorectal, <http://www.gastro.org/wmspage.cfm?parm1=686>
- [4] Chirtopher F. Beaulieu, R. Brooke Jeffrey, Chandu Karadi, David S. Paik, Sandy Napel, Display Modes For CT Colonography. Part II: Blinded Comparison Of Axial CT and Virtual Endoscopic and Panoramic Endoscopic Volume Rendered Studies, in RSNA Radiology, 1999.
- [5] Alberto Bert, Ivan Dmitriev, Silvano Agliozzo, Natalia Pietrosevoli, Mario Ferraro, Mark Mandelkern, Teresa Gallo, Daniele Regge, A new automatic method for colon segmentation in CT-Colonography CAD, 2003.
- [6] S. Bond, M. Brady, F. Gleeson, N. Mortesen, Image Analysis for Patient Management in Colorectal Cancer, in CARS, 2005.
- [7] Dongqing Chen, Zhengrong Liang, Mark R. Wax, Lihong Li, Bin Li, Arie E. Kaufman, A Novel Approach to Extract Colon Lumen from CT Images for Virtual Colonoscopy, in IEEE transactions on medical imaging, 2000.
- [8] Ming Wan, Frank Dacheille, Arie Kaufman, Distance-Field Based Skeletons for Virtual Navigation, in IEEE Visualization, 2001.
- [9] Leonardo Flórez, Modèle D'état De Cylindre Généralisé et la quantification de Sténoses Artérielles En Imagerie 3D, 2006.
- [10] Rafael C. Gonzalez, Richard E. Woods, Digital Image Processing, 2002.
- [11] Hounsfield Units, http://www.itk.org/Wiki/ITK_Hounsfield_Units
- [12] Peter W. Hung, David S. Paik, Sandy Napel, Judy Yee, R. Brooke Jeffrey, Andreas Steinauer-Gebauer, Juno Min, Ashwin Jathavedam, Christopher F. Beaulieu, Quantification of Distention in CT Colonography: Development and Validation of Three Computer Algorithms, in RSNA Radiology, 2002.
- [13] Gheorghe Iordanescu, Ronald M. Summers, Benefits of Centerline Analysis for CT Colonography Computer-Aided Polyp Detection, 2003.
- [14] Anna K. Jerebko, Sheldon B. Teerlink, Marek Franaszek, Ronald M. Summers, Polyp Segmentation Method for CT Colonography Computer Aided Detection, in SPIE , 2003.
- [15] Chandu Karadi, Chirtopher F. Beaulieu, R. Brooke Jeffrey, David S. Paik, Sandy Napel, Display Modes For CT Colonography. Part I: Synthesis And Insertion of Polypos into Pacient CT Data, in RSNA Radiology 1999.
- [16] Lihong Li, Dongqing Chen, Sarang Lakare, Kevin Kreeger, Ingmar Bitter, Arie E. Kaufman, Mark R. Wax, Petar M. Djuric, Zhengrong Liang, An image segmentation approach to extract colon lumen through colonic material tagging and hidden Markov random field model for virtual colonoscopy, in CiteSeer 2002.
- [17] Ping Li, Sandy Napel, Burak Acar, David S. Paik, R. Brooke Jeffrey, Christopher F. Beaulieu, Registration of central paths and colonic polyps between supine and prone scans in computed tomography colonography: Pilot study, in NCBI, 2004.
- [18] Wolfgang Luboldt, Peter Bauerfeind, Simon Wildermuth, Borut Marincek, Michael Fried, Jrg F. Debatin, Colonic Masses: Detection with MR Colonography, in RSNA Radiology, 2000.
- [19] R Mukundan, K R Ramakrishnan, Moment Functions In Image Analysis: Theory And Application, 1998.
- [20] David S. Paik, Christopher F. Beaulieu, Geoffrey D. Rubin, Burak Acar, R. Brooke Jeffrey, Jr., Judy Yee, Joyoni Dey, Sandy Napel, Surface Normal Overlap: A Computer-Aided Detection Algorithm With Application to Colonic Polyps and Lung Nodules in Helical CT, in IEEE transactions on medical imaging, 2004.
- [21] Joost F. Peters, Simona E. Griogorescu, Roel Truyen, Frans A. Gerritsen, Ayso H de Vries, Rogier E. van Gelder, Patrik Rogalla. Robust Automated Polyp Detection for low-dose and normaldose virtual colonoscopy, in Elsevier, 2005
- [22] Robert J.T. Sadleir, Paul F. Whelan, Colon Centerline Calculation for CT Colonography Using Optimised 3D Topological Thinning, in CiteSeer, 2002
- [23] Mie Sato, Sarang Lakare, Ming Wan, Arie Kaufman, Zhengrong Liang, mark Wax, An Automatic Colon Segmentation for 3d Virtual Colonoscopy, in IEICE Trans. Information and Systems 2001
- [24] Milan Sonka, Vaclav Hlavac, Roger Boyle, Image Processing, Analysis, and Machine Vision, 1999.

- [25] Ronald M. Summers, Christopher F. Beaulieu, Lynne M. Pusanik, James D Malley, R. Brooke, Jeffrey, Daniel I. Glazer, Sandy Napel, Automated Polyp Detector For CT Colonography: Feasibility Study, in RSNA Radiology, 2000
- [26] Ronald M. Summers, Anna K. Jerebko, Marek Franaszek, James D Malley, Daniel Johnson, Colonic Polyps: Complementary Role Of Computer Aided Detection In CT Colonography, in RNSA Radiology, 2002
- [27] Ronald M. Summers, Daniel Johnson, Lynne M. Pusanik, James D. Malley, Ashraf M. Youssef, Judd E. Reed, Automated Polyp Detection at CT Colonography: Feasibility Assessment in a Human Population. In RSNA Radiology, 2001.
- [28] Ming Wan, Zhengrong Liang, Qi Ke, Lichan Hong, Ingmar Bitter, Arie Kaufman, Automatic Centerline Extraction for Virtual Colonoscopy, in IEEE transactions on medical imaging, 2002
- [29] C.L. Wyatt, Y. Ge, D.J. Vining, Automatic segmentation of the colon for virtual colonoscopy, in Elsevier, 2000.
- [30] Jianhua Yao, Meghan Miller, Marek Franaszek, Ronald M. Summers, Automatic Segmentation of Colonic Polyps in CT Colonography Based on Knowledge-Guided Deformable Models. In SPIE, 2003